Carbohydrate Research 360 (2012) 78–83

Contents lists available at SciVerse ScienceDirect

Carbohydrate Research

journal homepage: www.elsevier.com/locate/carres

Non-symmetric liquid crystal dimer containing a carbohydrate-based moiety

Andrew G. Cook [a], James L. Wardell [a], Nicholas J. Brooks [b], John M. Seddon [b], Alfonso Martínez-Felipe [c], Corrie T. Imrie [a,*]

[a] Chemistry, School of Natural and Computing Sciences, University of Aberdeen, Meston Walk, Aberdeen AB24 3UE, UK
[b] Department of Chemistry, Imperial College of Science, Technology and Medicine, Exhibition Road, London SW7 2AY, UK
[c] Instituto de Tecnología de los Materiales (ITM), Universitat Politècnica de València (UPV) Camino de Vera S/N, 46022 Valencia, Spain

ARTICLE INFO

Article history:
Received 28 May 2012
Received in revised form 20 July 2012
Accepted 26 July 2012
Available online 3 August 2012

Keywords:
Liquid crystal dimer
Sugar
Smectic A phase
Variable temperature FTIR
Hydrogen bonding
Glassy behaviour

ABSTRACT

The synthesis and characterisation of a novel non-symmetric liquid crystal dimer, 1-[3-*O*-(D-glucopyranos-3-yl)]-8-[(4-methoxyazobenzene-4′-oxy)]octane is reported. This exhibits glassy behaviour and a highly interdigitated smectic A phase in which the aromatic and alkyl structural fragments overlap. Variable temperature infrared spectroscopy reveals that the strength and extent of hydrogen bonding within the system does not show a marked change at either the glass transition or at the smectic A-isotropic transition. This observation indicates that the smectic A-isotropic transition is driven by changes in the van der Waals interactions between the molecules while hydrogen bonded aggregates persist into the isotropic phase.

1. Introduction

There is now a wide range of low molar mass molecular architectures based on rod-like structures known to support liquid crystallinity[1] and of these, carbohydrate-based liquid crystals have attracted particular research attention.[2,3] This interest has arisen primarily for two reasons: firstly, the building blocks for these materials are numerous and inexpensive, and secondly, mesogenic monosaccharides and polysaccharides play an important role in many biological processes.[4,5] A carbohydrate-based mesogen typically consists of a hydrophilic (polar) head group attached to which are one or more lipophilic (nonpolar) chains. These amphiphilic molecules have a strong tendency to microphase separate into two distinct microdomains, one composed of the polar sugar moieties and the other, the nonpolar alkyl chains, typically yielding interdigitated smectic A behaviour.[4]

Carbohydrate-based liquid crystals are immiscible with conventional thermotropic low molar mass liquid crystals which contain molecules comprising a single semi-rigid core, normally consisting of phenyl rings connected by short unsaturated linkages, attached to which are one or two flexible alkyl chains.[6,7] In essence, in these so-called conventional systems, the anisotropic interactions between the semi-rigid cores give rise to liquid crystallinity while the role of the alkyl chains is largely to reduce the melting point of the material. For a great many years it was widely believed that low molar mass liquid crystals actually required molecules containing a semi-rigid core although this is no longer the case.[1] Indeed, liquid crystal dimers which consist of molecules comprised of two mesogenic groups connected via a flexible spacer, normally an alkyl chain, represent an inversion of the conventional architecture and have been the focus of considerable research attention.[8–10]

Of particular interest are non-symmetric liquid crystal dimers in which the molecules contain two different liquid crystal groups connected by a flexible spacer.[9] In the overwhelming majority of non-symmetric dimers, the two mesogenic groups are chosen with the expectation that they will exhibit a specific favourable interaction and this design approach led to the discovery of the intercalated smectic phases.[11–14] However, this molecular architecture has also been exploited to combine immiscible liquid crystal groups; for example, rod-like and disc-like moieties have been connected through flexible spacers.[15–17]

Molecular architectures which combine the structural elements of cyclic carbohydrates and conventional rod-like low molar mass mesogens linked by flexible spacers are rare; examples include, liquid crystal trimers consisting of two glucopyranoside groups and a central diphenylbutadiene or azobenzene unit linked by two flexible spacers,[18,19] a non-symmetric dimer containing a sugar and steroid unit,[20] and star-shaped compounds with a carbohydrate-based core and peripheral conventional mesogenic side chains.[21–26]

* Corresponding author. Tel.: +44 1224 272567; fax: +44 1224 273105.
E-mail address: c.t.imrie@abdn.ac.uk (C.T. Imrie).

0008-6215
http://dx.doi.org/10.1016/j.carres.2012.07.018

Recently, Yoshizawa described the properties of a non-symmetric dimer in which a phenylpyrimidine and D-glucamine were connected by an alkyl spacer and this showed cytostatic activity against A549 human lung carcinoma cell lines.[27] To our knowledge, however, there have been no reports of a non-symmetric dimer in which a conventional mesogenic core and a cyclic monosaccharide are connected via a flexible spacer, and thus, we prepared 1-[3-*O*-(D-glucopyranos-3-yl)]-8-[(4-methoxyazobenzene-4′-oxy)]octane, **1**, and have characterised its liquid crystalline properties.

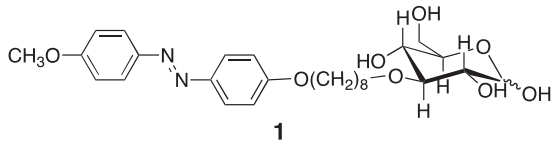

1

2. Experimental

Compound **1** was prepared using the synthetic route shown in Scheme 1. The syntheses of 4-methoxy-4′-hydroxyazobenzene, **2**,[28] 1-bromo-8-(4-methoxyazobenzene-4′-oxy)octane, **3**,[29] and 1,2:5,6-di-*O*-isopropylidene-α-D-glucofuranose, **4**,[30] have been described in detail elsewhere.

2.1. Synthesis of 1-[3-*O*-(1,2:5,6-di-*O*-isopropylidene-α-D-glucofuranos-3-yl)]-8-[(4-methoxyazobenzene-4′-oxy)]octane, 5

Compound **5** was prepared using the method described by Bessodes et al.[31] Thus, freshly powdered potassium hydroxide (1 g, 17.9 mmol) and 18-crown-6 (0.11 g, 0.4 mmol), were added to a solution of 1,2:5,6-di-*O*-isopropylidene-α-D-glucofuranose, **4**, (2.36 g, 9 mmol) and 1-bromo-8-(4-methoxyazobenzene-4′-oxy)-octane, **3**, (4.19 g, 10 mmol) in THF (20 ml). The mixture was stirred at room temperature overnight, diluted with CH_2Cl_2, and washed several times with water. The organic phase was evaporated under reduced pressure and the alkylated product was purified by column chromatography (elute 7:3 hexane/ethyl acetate). Yield 45%. ^{1}H NMR ($CDCl_3$) δ (ppm): 1.17–1.60 (m, 22H, (12H, CH_3 isopropylidiene groups), (10H, spacer CH_2)), 1.80 (m, 2H, OCH_2CH_2), 3.53 (m, 2H, OCH_2), 3.9 (s, 3H, OCH_3), 3.91–4.17 (m, 6H, (2H, OCH_2), (4H on sugar)), 4.30 (qt, 1H, on sugar), 4.50 (d, 1H, CH), 5.85 (d, 1H, H_1), 6.95, 7.84 (m, 8H, aromatic).

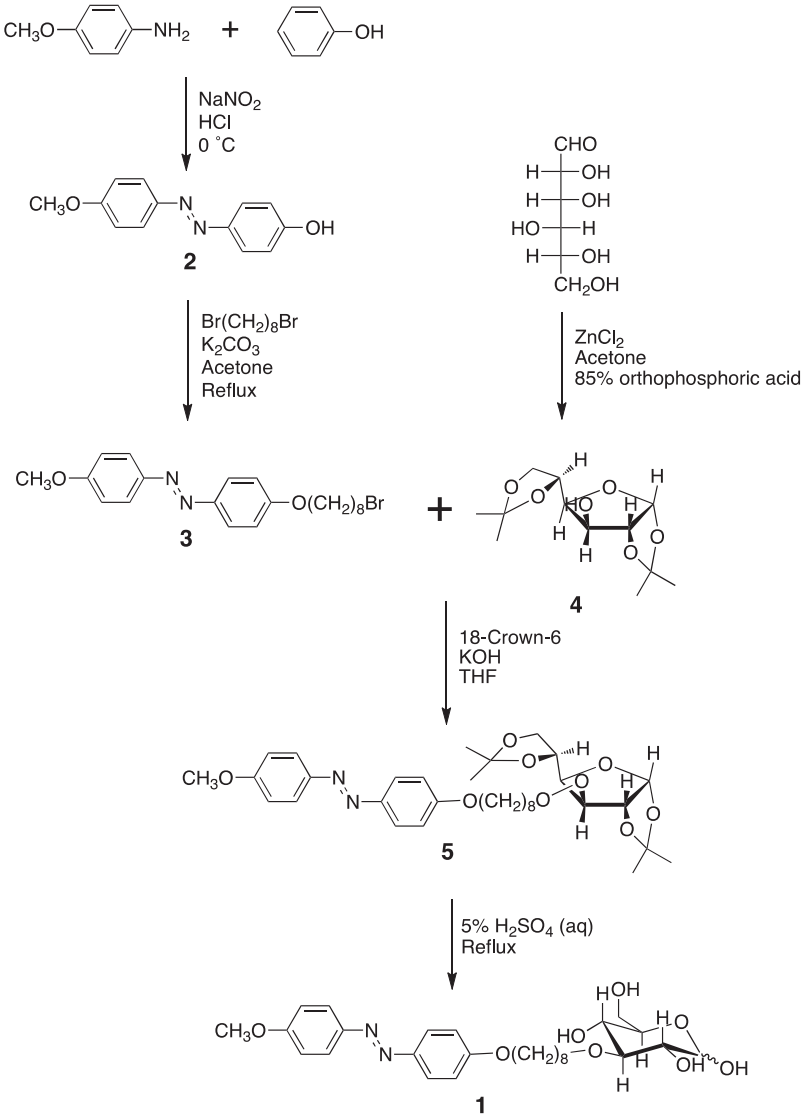

Scheme 1. Synthesis of 1-[3-*O*-(D-glucopyranos-3-yl)]-8-[(4-methoxyazobenzene-4′-oxy)]octane, **1**.

2.2. Synthesis of 1-[3-*O*-(D-glucopyranos-3-yl)]-8-[(4-methoxyazobenzene-4′-oxy)]octane, 1

1-[3-*O*-(1,2:5,6-Di-*O*-isopropylidene-α-D-glucofuranos-3-yl)]-8-[(4-methoxyazobenzene-4′-oxy)]octane, **5**, (1 g) was refluxed for 8 h in 5% sulphuric acid solution (10 ml). The hydrolysate was washed with chloroform and water in a separating funnel. The insoluble material was removed by filtration and recrystallised from ethanol. The ^{1}H NMR spectrum of this yellow solid obtained in DMSO-d_6 confirmed it to be the deprotected sugar, **1**.

Yield 60%. Elemental analysis: anal. calcd for $C_{27}H_{38}N_2O_8$: C, 62.51; H, 7.39; N, 5.40. Found: C, 62.22; H, 7.17; N, 5.36. ^{1}H NMR (DMSO-d_6) δ (ppm): 1.29 (m, 6H, CH_2CH_2), 1.40 (m, 2H, CH_2CH_2), 1.48 (m, 2H, CH_2CH_2), 1.72 (m, 2H, $ArOCH_2CH_2$), 3.13 (m, H_3), 3.22 (t, 2H, J = 5.9 Hz, OCH_2), 3.40 (m, 2 H_6), 3.66 (m, H_2, H_4, H_5) 3.84 (s, 3H, OCH_3), 4.02 (t, 2H, J = 6.5 Hz, $ArOCH_2$), 6.60 (br s, 1H, H_1), 7.10 (m, 4H, aromatic), 7.82 (m, 4H, aromatic).). IR (KBr) ν cm^{-1}: 3442 (O–H stretching), 1600, 1582 and 1500 cm^{-1} (aromatic C–C stretching), 1250 (C–O–C stretching).

2.3. Characterisation

The structures of **1** and all intermediates were verified by ^{1}H NMR spectroscopy using Varian Unity Inova 400 MHz and Bruker AC-F 250 MHz spectrometers, and by FTIR spectroscopy using an ATI Mattson spectrometer. Elemental analysis of **1** was performed by Butterworth Laboratories Ltd. The transitional properties of **1** were determined by differential scanning calorimetry (DSC) in a nitrogen atmosphere using a Mettler-Toledo DSC821e differential scanning calorimeter cooled by liquid nitrogen and calibrated using indium and zinc as standards. The time–temperature programme used for the DSC analyses was (i) an initial heat from −20 to 180 °C at 10 °C/min; (ii) held for 3 min at 180 °C; (iii) cooled from 180 to −20 °C at 10 °C/min; (iv) held for 3 min at −20 °C and (v) reheated from −20 to 180 °C at 10 °C/min. The thermodynamic data quoted are averaged values from measurements of two aliquots of **1** and extracted from the reheating traces. Phase identification was performed by polarised light microscopy using an Olympus BH-2 optical microscope equipped with a Linkam TMHS 600 heating stage and a TMS 92 control unit. The molecular arrangement within the liquid crystal phase was probed using X-ray diffraction using a Huber X-ray camera, the calibration of which was checked using silver behenate (d = 58.3 Å) and found to be correct within 0.1 Å. The X-ray experiments were performed on two different samples and the results found to be identical. The FT-IR spectrum of **1** as a function of temperature was obtained using a Nicolet Nexus FT-IR bench attached to a Continuum FT-IR microscope equipped with a Linkam FT-IR 600 heating stage and a TMS 93 control unit. The sample was sandwiched between a gold-coated microscope slide and a 3 mm KBr disc. A thin film of the sample was obtained by first heating it into the isotropic phase. The spectra were recorded on subsequent reheating in a trans-reflectance mode that is the IR beam passed through the sample was reflected by the gold surface back through the sample and then detected.

3. Results and discussion

Figure 1 shows the traces obtained for the heat–cool–heat DSC cycle of **1**. In the first heating, a rather broad endotherm is seen at about 67.5 °C followed by a second endotherm at 167 °C (Fig. 1a). On cooling, an exotherm with onset temperature of 165 °C is observed followed by a second order transition with a mid-point at 86 °C (Fig. 1b). On subsequent reheating, a second order transition with a mid-point at 88 °C is followed by an endotherm at 165 °C

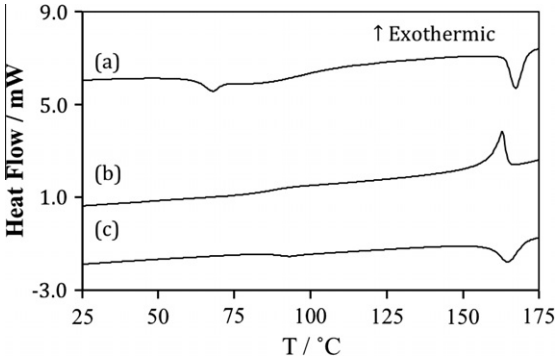

Figure 1. The DSC traces obtained for **1**: (a) first heating, (b) cooling and (c) second heating. The traces have been arbitrarily displaced along the y-axis for the sake of clarity.

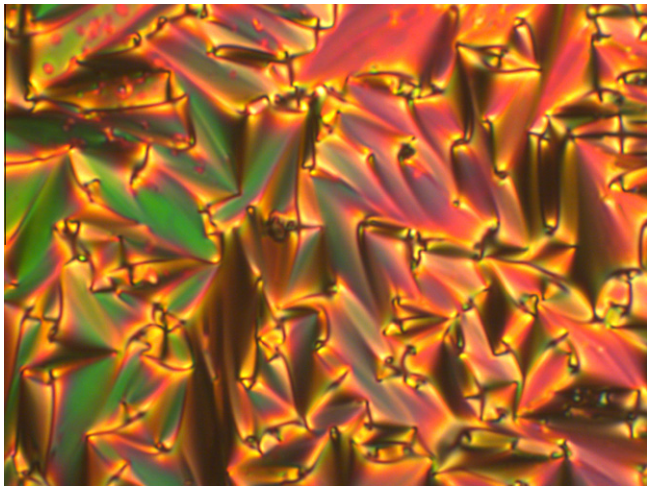

Figure 2. The focal conic fan texture seen for the smectic A phase exhibited by **1** at 156 °C.

(Fig. 1c). We note that on repeated cycling the transition temperatures decrease and the associated peaks increase in breadth. This is indicative of sample decomposition.

On cooling from the isotropic phase, bâtonnets developed which coalesce to give a focal conic fan texture (Fig. 2) in co-existence with regions of homeotropic alignment when viewed through the polarised light microscope. The presence of focal conic fans implies a layered structure, while the homeotropic alignment indicates an orthogonal arrangement of the director with respect to the layer planes. Thus, the phase is assigned as a smectic A phase. The texture remains unchanged on cooling to room temperature and thus the lower temperature second order transition is assigned as a glass transition. The smectic A-isotropic assignment is supported by the value measured for the entropy change associated with the smectic A-isotropic transition, expressed as the dimensionless quantity $\Delta S/R$, of 3.23 which is comparable to that seen for the smectic A-isotropic transition shown by other symmetric and non-symmetric liquid crystal dimers.[32,33]

The X-ray diffraction powder pattern of the smectic A phase of **1** is shown in Figure 3 and confirmed this assignment. Thus, in the low angle region of the X-ray diffraction pattern of the smectic A phase, two sharp peaks of similar intensities were observed in the spacing ratio 1:2 at a spacing, d, of 31.7 Å, while in the wide angle region, a diffuse peak was seen centred at ca. 4.3 Å characteristic of a liquid-like arrangement of the molecules within the layers. In the low angle region of the X-ray pattern of the smectic A glass,

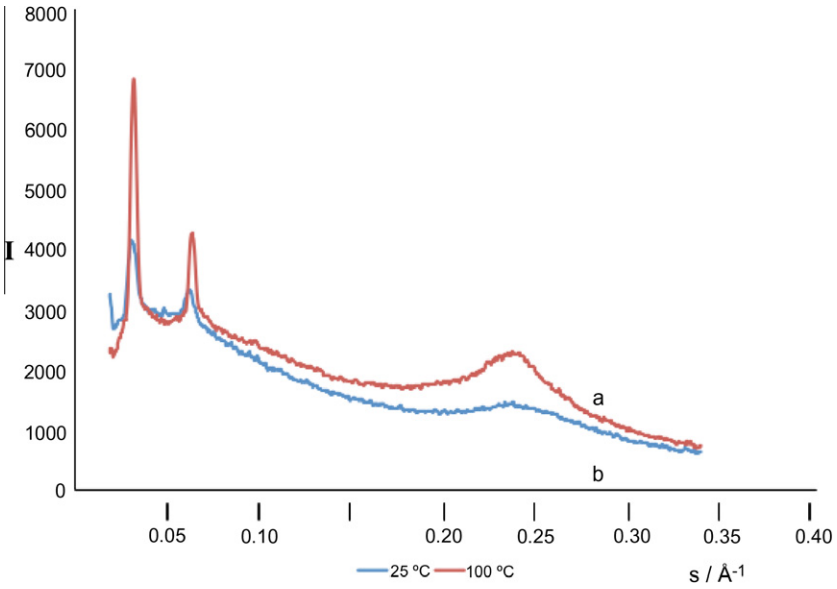

Figure 3. X-ray patterns of (a) the smectic A phase at 100 °C, and (b) the smectic A glass at 25 °C.

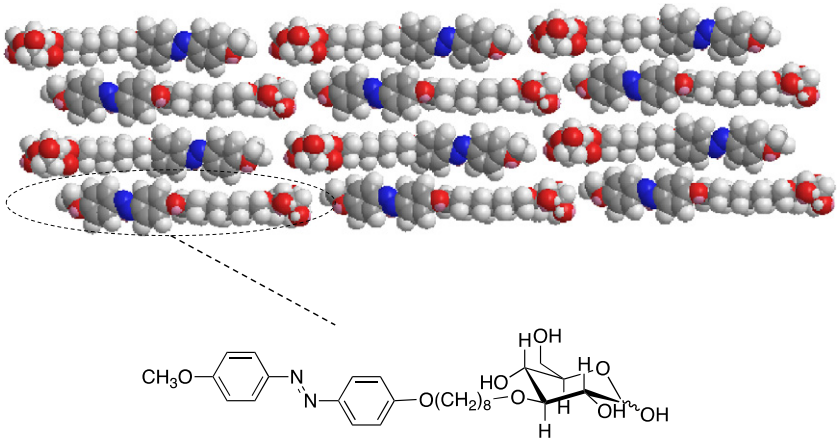

Figure 4. A sketch of the molecular organisation within the interdigitated smectic A phase shown by **1**.

two slightly diffuse peaks of similar intensities, in the spacing ratio 1:2 at a spacing of 31.8 Å are seen while in the wide angle region a diffuse peak is observed centred at ca. 4.3 Å On heating the sample from 50 °C to 150 °C at 10 °C/h, the X-ray diffraction pattern is essentially unchanged with only a sharpening of the low angle peaks into Bragg peaks at ca. 95 °C which corresponds to the glass transition detected using DSC. The low angle spacing decreases by ca. 0.5 Å over this temperature range while the diffuse wide-angle peak appears unchanged over the whole temperature range. The estimated molecular length, *L*, is 27.5 Å such that the ratio of the smectic periodicity to molecular length, *d*/*L*, is 1.15, suggesting that the smectic phase must have an interdigitated structure in which the alkyl chains and aromatic cores overlap considerably. Figure 4 shows a sketch of the molecular organisation within the smectic A phase consistent with this *d*/*L* value and this is similar to the structure of the smectic A phase proposed for steroidal glycolipids.[34] We shall discuss the structure of the smectic A phase in more detail later.

The liquid crystal behaviour of carbohydrate-based materials is most commonly attributed to hydrogen bonding between the carbohydrate moieties[35] and this can be conveniently investigated using FT-IR spectroscopy. Thus, Figure 5 shows the infrared spectrum of the non-symmetric dimer **1** in the glass, smectic A and isotropic phases. The band associated with O–H stretching is often used as a test for, and a measure of, the extent and strength of hydrogen bonding within a system. Thus, a free O–H group gives rise to a strong and sharp band in the 3650–3590 cm^{-1} region while involvement in hydrogen bonding shifts this to lower frequency and it generally becomes much broader. In the glass, the O–H stretching band is centred at 3456 cm^{-1}. On heating the sample into the smectic A phase, the band shifts to 3472 cm^{-1} and on further heating can be seen at 3526 cm^{-1} in the isotropic phase. These shifts point to a reduction in the strength of hydrogen bonding on increasing temperature.

The temperature dependence of the O–H stretching peak is more easily visualised in Figure 6 which shows this region of the spectrum as a function of temperature on heating while Figure 7 shows the dependence of the peak position on temperature.

Figure 7 shows that the position of the O–H stretching peak appears to vary linearly with temperature but with kinks coinciding approximately with the glass and smectic A-isotropic transition temperatures. In the glass phase, the gradient of the line of best fit is 0.32 cm^{-1}/K, in the SmA phase 0.49 cm^{-1}/K, and in the isotropic phase 1.46 cm^{-1}/K. Wolkers et al.[36,37] termed these gradients

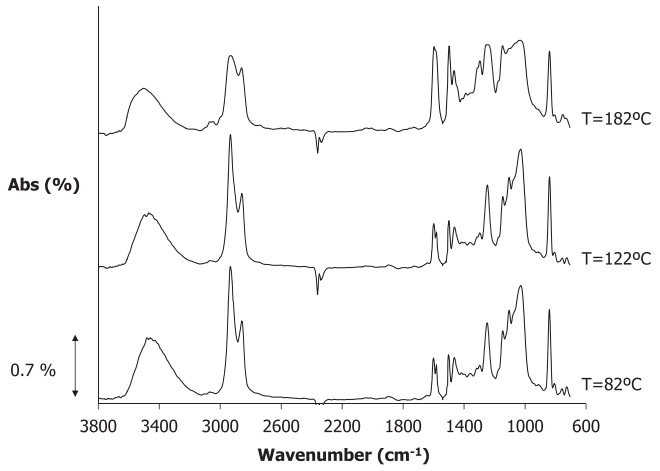

Figure 5. Infrared spectra for **1** measured in the glass (82 °C), smectic A (122 °C) and isotropic phases (182 °C). The spectra have been shifted arbitrarily along the *y*-axis for the sake of clarity.

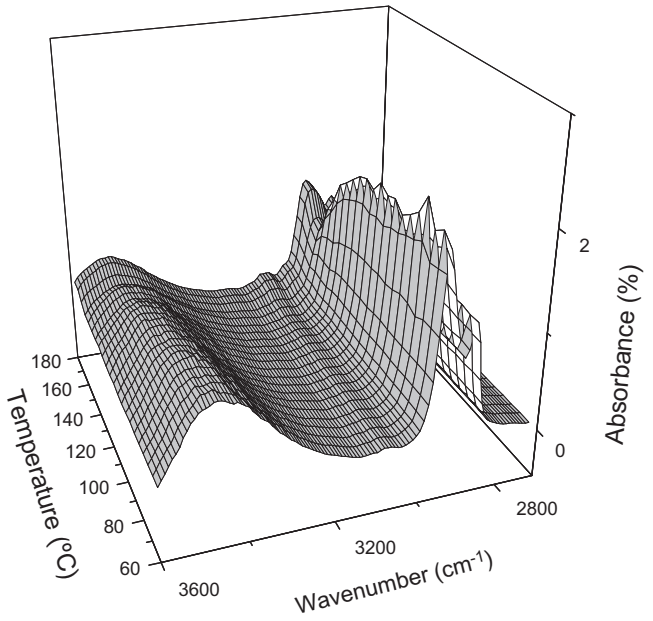

Figure 6. The dependence of the 3600–2800 cm^{-1} region of the infrared spectra of **1** on temperature. The spectra have been recorded on heating from the glass phase.

wavenumber–temperature coefficients (WTC) and measured them for a range of amorphous sugars above and below the glass transition. To our knowledge, the values reported here are the first to be given for a sugar-based liquid crystal. In the glass phase Wolkers reported WTC values in the range of 0.1–0.45 cm^{-1}/K, and in the liquid phase 0.48–0.60 cm^{-1}/K.[36] A small change in WTC at the glass transition implies only small changes in the hydrogen bonding network and correlated with a small ΔC_p at T_g. Conversely, a large change in WTC at the glass transition was associated with large values of ΔC_p at T_g. In terms of Angell's concept of strength and fragility, a larger change in WTC at the glass transition corresponds to an increase in fragility and a loss of strength in the system.[38]

For the non-symmetric dimer **1**, the change in WTC at T_g is ca. 0.17 cm^{-1}/K^{-1}, which is smaller than any of the values reported by Wolkers et al.[37] for amorphous sugar glasses. The value of ΔC_p for the glass transition of **1** is 0.37 J g^{-1} K^{-1} and is similar to that seen for the strongest of the amorphous glasses.[37] This indicates that the structure of the smectic A phase changes little on vitrification. The absence of a step change in the position of the O–H stretching peak at T_g was interpreted by Ottenhof et al.[39] as indicating that a threshold of hydrogen bond strength and density is reached which results in the decrease in molecular mobility yielding vitrification.

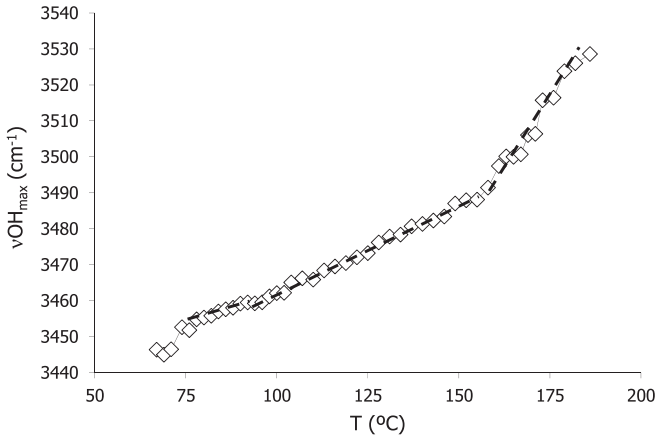

Figure 7. The dependence of the O–H stretching peak position in the infrared spectra of **1** on temperature.

By contrast a much larger change is observed in WTC around the smectic A-isotropic transition (Fig. 7). Surprisingly, however, no step change is observed in the position of the O–H stretching peak at the clearing point even thought the structure of the material changes significantly. In comparison, cold crystallisation in conventional sugars is accompanied by a step change in the position of the O–H peak, the magnitude of which appears to be linked to the size of the crystallisation enthalpy.[39] This indicates that the strength and density of the hydrogen bonding in the smectic A phase exhibited by **1** does not change significantly at the smectic A-isotropic transition. A similar observation has been reported for a conventional carbohydrate-based liquid crystal.[40]

It is also apparent in Figure 5 that the bands at ca. 1600 cm^{-1} and 1500 cm^{-1} associated with vibrations of the aromatic ring increase in intensity on increasing temperature. This may be accounted for in terms of a change in alignment of the sample on increasing temperature. Specifically, the incident IR beam is polarised on reflection at the gold surface[41] and so vibrations parallel to the surface will not be detected. On cooling, the non-symmetric dimer tends to adopt homeotropic alignment and hence, the intensity of the bands associated with the in-plane vibrations of the aromatic rings will decrease.

If we now consider the transitional properties of the two symmetric dimers, then 1,8-bis[(4-methoxyazobenzene-4′-oxy)]octane, **6**,

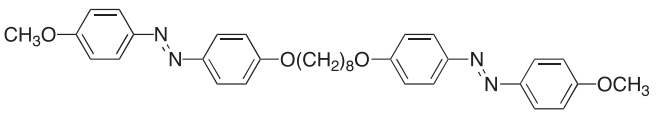

melts into the nematic phase at 199 °C, undergoes a nematic-isotropic transition at 217 °C with an associated entropy change, $\Delta S_{NI}/R$, of 1.76.[42] The symmetric bolaamphiphile, 1,8-bis[3-*O*-(D-glucopyranos-3-yl)]octane, **7**,

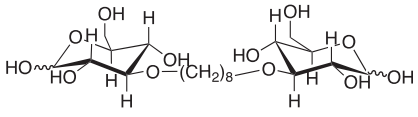

does not exhibit liquid crystalline behaviour and melts directly into the isotropic phase between 143 and 145 °C.[43] Thus, the nematic behaviour of the conventional calamitic symmetric dimer has been extinguished while the tendency of the sugar-based symmetric dimer to crystallise has been inhibited in the non-symmetric dimer.

The injection of smectic behaviour is presumably a consequence of the incompatibility of the two mesogenic units in **1**. This cannot give rise to a monolayer smectic A phase, however, as there exists a mismatch in the cross-sectional areas of the three structural components, that is, the azobenzene-based mesogenic group, the sugar and the alkyl spacer. Thus, to fill space effectively the azobenzene-based unit must overlap with the alkyl spacer and this is consistent with the smectic periodicity measured using X-ray diffraction. The smectic arrangement, therefore, consists of a highly interdigitated arrangement with the sugar groups on the outside of the layer and the alkyl spacer and the azobenzene-based mesogenic overlapping in the centre of the layer (see Fig. 4). This overlap between the aromatic and alkyl groups is unfavourable and in conventional dimers drives the formation of smectic phases.[32] Presumably the hydrogen bonding between the sugar groups overcomes these unfavourable interactions and lamellar-like behaviour results from the matching of the cross-sectional areas of the sugar region and the alkyl-aromatic region.

4. Conclusions

The liquid crystalline behaviour of the non-symmetric dimer, 1-[3-*O*-(D-glucopyranos-3-yl)]-8-[(4-methoxyazobenzene-4′-oxy)]-octane, in which a conventional rod-like azobenzene-based mesogenic unit is attached via a flexible alkyl spacer to a cyclic monosaccharide has been reported. The dimer exhibits a highly interdigitated smectic A phase in which the aromatic and alkyl units overlap. There is no step change in the strength and extent of hydrogen bonding at the smectic A-isotropic transition implying that hydrogen bonding, although important in stabilising the layer arrangement, does not in fact drive the formation of the phase. Instead it is presumably the change in the van der Waals interactions between the molecules at the clearing temperature which destroys the smectic arrangement while hydrogen bonded aggregates remain intact. It is surprising, however, that the entropy change associated with the smectic A-isotropic transition is comparable to that observed for conventional liquid crystal dimers. By comparison, for other carbohydrate-based liquid crystals[40] and ionic liquid crystals[44] for which aggregates are thought to persist into the isotropic phase, the entropy change at the clearing point is very small. The physical significance of this observation is not clear. The molecular arrangement within the smectic A layers shown by **1** is stabilised by the matching of the cross-sectional areas of the sugar region and the alkyl-aromatic region. If, however, such packing is prevented we anticipate that interfacial curvature will give rise to a range of novel phase behaviour and this now warrants further study.

Acknowledgments

J.M.S. is pleased to acknowledge support from the EPSRC Platform Grant EP/G00465X and A.M.F from the Grisolia Program from Generalitat Valenciana.

References

1. Goodby, J. W.; Saez, I. M.; Cowling, S. J.; Gasowska, J. S.; MacDonald, R. A.; Sia, S.; Watson, P.; Toyne, K. J.; Hird, M.; Lewis, R. A.; Lee, S. E.; Vaschenko, V. *Liq. Cryst.* **2009**, *36*, 567–605.
2. Brooks, N. J.; Hamid, H. A. A.; Hashim, R.; Heidelberg, T.; Seddon, J. M.; Conn, C. E.; Husseini, S. M. M.; Zahid, N. I.; Hussen, R. S. D. *Liq. Cryst.* **2011**, *38*, 1725–1734.
3. Hashim, R.; Sugimura, A.; Minamikawa, H.; Heidelberg, T. *Liq. Cryst.* **2012**, *39*, 1–17.
4. Goodby, J. W.; Gortz, V.; Cowling, S. J.; Mackenzie, G.; Martin, P.; Plusquellec, D.; Benvegnu, T.; Boullanger, P.; Lafont, D.; Queneau, Y.; Chambert, S.; Fitremann, J. *Chem. Soc. Rev.* **2007**, *36*, 1971–2032.
5. Jewell, S. A. *Liq. Cryst.* **2011**, *38*, 1699–1714.
6. Goodby, J. W. *Liq. Cryst.* **2011**, *38*, 1363–1387.
7. Hird, M. *Liq. Cryst.* **2011**, *38*, 1467–1493.
8. Imrie, C. T.; Henderson, P. A. *Curr. Opin. Colloid Interface Sci.* **2002**, *7*, 298–311.
9. Imrie, C. T.; Henderson, P. A. *Chem. Soc. Rev.* **2007**, *36*, 2096–2124.
10. Imrie, C. T.; Henderson, P. A.; Yeap, G. Y. *Liq. Cryst.* **2009**, *36*, 755–777.
11. Hogan, J. L.; Imrie, C. T.; Luckhurst, G. R. *Liq. Cryst.* **1988**, *3*, 645–650.
12. Attard, G. S.; Date, R. W.; Imrie, C. T.; Luckhurst, G. R.; Roskilly, S. J.; Seddon, J. M.; Taylor, L. *Liq. Cryst.* **1994**, *16*, 529–581.
13. Imrie, C. T. *Liq. Cryst.* **2006**, *33*, 1449–1454.
14. Yeap, G. Y.; Hng, T. C.; Yeap, S. Y.; Gorecka, E.; Ito, M. M.; Ueno, K.; Okamoto, M.; Mahmood, W. A. K.; Imrie, C. T. *Liq. Cryst.* **2009**, *36*, 1431–1441.
15. Fletcher, I. D.; Luckhurst, G. R. *Liq. Cryst.* **1995**, *18*, 175–183.
16. Date, R. W.; Bruce, D. W. *J. Am. Chem. Soc.* **2003**, *125*, 9012–9013.
17. Imrie, C. T.; Lu, Z.; Picken, S. J.; Yildirim, Z. *Chem. Commun.* **2007**, 1245–1247.
18. Abraham, S.; Paul, S.; Narayan, G.; Prasad, S. K.; Rao, D. S. S.; Jayaraman, N.; Das, S. *Adv. Funct. Mater.* **2005**, *15*, 1579–1584.
19. Das, S.; Gophinathan, N.; Abraham, S.; Jayaraman, N.; Singh, M. K.; Prasad, S. K.; Rao, D. S. S. *Adv. Funct. Mater.* **2008**, *18*, 1632–1640.
20. Rachedi, F. A.; Chambert, S.; Ferkous, F.; Queneau, Y.; Cowling, S. J.; Goodby, J. W. *Chem. Commun.* **2009**, 6355–6357.
21. Zhang, B. Y.; Xiao, W. Q.; Cong, Y. H.; Zhang, Y. H. *Liq. Cryst.* **2007**, *34*, 1129–1136.
22. Xiao, W. Q.; Zhang, B. Y.; Cong, Y. H. *Chem. Lett.* **2007**, *36*, 938–939.
23. Akiyama, H.; Tanaka, A.; Hiramatsu, H.; Nagasawa, J.; Tamaoki, N. *J. Mater. Chem.* **2009**, *19*, 5956–5963.
24. Tian, M.; Zhang, B.-Y.; Cong, Y.-H.; He, X.-Z.; Chu, H.-S.; Zhang, X.-Y. *Liq. Cryst.* **2010**, *37*, 1373–1379.
25. Belaissaoui, A.; Cowling, S. J.; Saez, I. M.; Goodby, J. W. *Soft Matter* **2010**, *6*, 1958–1963.
26. Belaissaoui, A.; Saez, I. M.; Cowling, S. J.; Zeng, X.; Goodby, J. W. *Chem. Eur. J.* **2012**, *18*, 2366–2373.
27. Yoshizawa, A.; Takahashi, Y.; Terasawa, R.; Chiba, S.; Takahashi, K.; Hazawa, M.; Kashiwakura, I. *Chem. Lett.* **2009**, *38*, 310–311.
28. Stewart, D.; Imrie, C. T. *Polymer* **1996**, *37*, 3419–3425.
29. Imrie, C. T.; Karasz, F. E.; Attard, G. S. *Macromolecules* **1992**, *25*, 1278–1283.
30. Glen, W. L.; Myers, G. S.; Grant, G. A. *J. Chem. Soc.* **1951**, 2568–2572.
31. Bessodes, M.; Shamsazar, J.; Antonakis, K. *Synthesis* **1988**, *7*, 560–562.
32. Date, R. W.; Imrie, C. T.; Luckhurst, G. R.; Seddon, J. M. *Liq. Cryst.* **1992**, *12*, 203–238.
33. Attard, G. S.; Garnet, S.; Hickman, C. G.; Imrie, C. T.; Taylor, L. *Liq. Cryst.* **1990**, *7*, 495–508.
34. Chambert, S.; Doutheau, A.; Queneau, Y.; Cowling, S. J.; Goodby, J. W.; Mackenzie, G. J. *Carbohydr. Chem.* **2007**, *26*, 27–39.
35. Goodby, J. W.; Watson, M. J.; Mackenzie, G.; Kelly, S. M.; Bachir, S.; Bault, P.; Gode, P.; Goethals, G.; Martin, P.; Ronco, G.; Villa, P. *Liq. Cryst.* **1998**, *25*, 139–147.
36. Wolkers, W. F.; Oldenhof, H.; Alberda, M.; Hoekstra, F. A. *Biochim. Biophys. Acta* **1998**, *1379*, 83–96.
37. Wolkers, W. F.; Oliver, A. E.; Tablin, F.; Crowe, J. H. *Carbohydr. Res.* **2004**, *339*, 1077–1085.
38. Angell, C. A.; Imrie, C. T.; Ingram, M. D. *Polym. Int.* **1998**, *47*, 9–15.
39. Ottenhof, M. A.; MacNaughtan, W.; Farhat, I. A. *Carbohydr. Res.* **2003**, *338*, 2195–2202.
40. Cook, A. G.; Wardell, J. L.; Imrie, C. T. *Chem. Phys. Lipids* **2011**, *164*, 118–124.
41. Coats, A. M.; Hukins, D. W. L.; Imrie, C. T.; Aspden, R. M. *J. Microsc.* **2003**, *211*, 63–66.
42. Henderson, P. A.; Cook, A. G.; Imrie, C. T. *Liq. Cryst.* **2004**, *31*, 1427–1434.
43. Gouéth, P.; Ramiz, A.; Ronco, G.; Mackenzie, G.; Villa, P. *Carbohydr. Res.* **1995**, *266*, 171–189.
44. De Roche, J.; Gordon, C. M.; Imrie, C. T.; Ingram, M. D.; Kennedy, A. R.; Lo Celso, F.; Triolo, A. *Chem. Mater.* **2003**, *15*, 3089–3097.